



NRC Publications Archive Archives des publications du CNRC

Use of Infrared Spectroscopy to Characterize Clay Intercalation and Exfoliation in Polymer Nanocomposites

Cole, Kenneth

This publication could be one of several versions: author's original, accepted manuscript or the publisher's version. / La version de cette publication peut être l'une des suivantes : la version prépublication de l'auteur, la version acceptée du manuscrit ou la version de l'éditeur.

For the publisher's version, please access the DOI link below. / Pour consulter la version de l'éditeur, utilisez le lien DOI ci-dessous.

Publisher's version / Version de l'éditeur:

<http://dx.doi.org/10.1021/ma0628329>

Macromolecules, 41, 3, pp. 834-843, 2008

NRC Publications Record / Notice d'Archives des publications de CNRC:

<http://nparc.cisti-icist.nrc-cnrc.gc.ca/npsi/ctrl?action=rtdoc&an=11230058&lang=en>

<http://nparc.cisti-icist.nrc-cnrc.gc.ca/npsi/ctrl?action=rtdoc&an=11230058&lang=fr>

Access and use of this website and the material on it are subject to the Terms and Conditions set forth at

http://nparc.cisti-icist.nrc-cnrc.gc.ca/npsi/jsp/nparc_cp.jsp?lang=en

READ THESE TERMS AND CONDITIONS CAREFULLY BEFORE USING THIS WEBSITE.

L'accès à ce site Web et l'utilisation de son contenu sont assujettis aux conditions présentées dans le site

http://nparc.cisti-icist.nrc-cnrc.gc.ca/npsi/jsp/nparc_cp.jsp?lang=fr

LISEZ CES CONDITIONS ATTENTIVEMENT AVANT D'UTILISER CE SITE WEB.

Contact us / Contactez nous: nparc.cisti@nrc-cnrc.gc.ca.



IMI 2007-116591-9
CNRC 49626.

The Use of Infrared Spectroscopy to Characterize Clay Intercalation and Exfoliation in Polymer Nanocomposites

*Kenneth C. Cole**

National Research Council Canada, Industrial Materials Institute, 75 De Mortagne Blvd., Boucherville,
Quebec, Canada J4B 6Y4

kenneth.cole@imi.cnrc-nrc.gc.ca

Received

Clay Exfoliation by Infrared Spectroscopy

ABSTRACT: The use of infrared spectroscopy as a technique for characterizing the state of intercalation and exfoliation in polymer nanocomposites prepared from montmorillonite-based nanoclays was investigated. The nanocomposite samples were based on polypropylene (blown films) or high density polyethylene (extruded material). It was clearly shown that the shape of the clay band envelope in the 1300-750 cm^{-1} region, which includes four Si-O stretching modes, varies with the degree of processing and is sensitive to the quality of intercalation/exfoliation. Peak fitting was used to elucidate the nature of the changes and to develop quantitative indicators. The out-of-plane Si-O mode near 1070 cm^{-1} is particularly sensitive and undergoes significant shifts in frequency. Infrared spectroscopy is a valuable complement to established techniques like X-ray diffraction and transmission electron microscopy, and has the added advantage of being able to provide a relatively fast indication of

the overall degree of intercalation/exfoliation, including clay particles with interlayer spacings outside the range of X-ray diffraction. Furthermore, it offers the possibility of use as a quality control method, either in the laboratory or on-line.

Introduction

Polymer nanocomposites based on layered silicate reinforcement materials continue to attract considerable attention. These reinforcements, which may be naturally occurring (for example, montmorillonite clay) or synthetic, possess a structure consisting of negatively-charged aluminosilicate layers less than 1 nm thick, closely associated in stacks, with counterbalancing cations like sodium along with loosely bound water molecules located in the space between the layers. By appropriate treatment, the metal cations can be replaced by larger organic ions (intercalants) that increase somewhat the interlayer distance. The most common intercalants are quaternary ammonium ions bearing at least one relatively long hydrocarbon chain. When such organoclays are dispersed in a polymer or a polymer precursor, further intercalation can occur and in ideal circumstances will lead to complete separation of the layers, or exfoliation. The result is a very efficient reinforcing effect, because the layers are highly anisometric (1 nm thick and hundreds of nm in diameter) and a relatively small amount of clay can give rise to a very large number of particles with a correspondingly large surface area. Consequently, less than five percent of clay by weight can produce significant improvements in various properties (mechanical, barrier, fire retardancy, etc.) with little adverse effect on transparency and density.

Since the improvements in properties are directly related to the quality of clay intercalation and exfoliation, it is important to properly characterize the degree of layer separation. The two techniques commonly used for this purpose are X-ray diffraction (XRD) at small angles ($2\theta < 10^\circ$) and transmission electron microscopy (TEM). Both provide useful information, but even together they do not give a complete picture. XRD data typically show a peak whose position is related to the interlayer spacing d_{001} through the Bragg relationship $d_{001} = \lambda / (2 \sin \theta)$. The peak maximum thus corresponds to the most probable spacing, and its broadness can give some idea of the distribution of spacings, although

it is also related to other factors. Careful sample preparation, experimental technique, and data interpretation are necessary if reliable information is to be obtained from XRD.¹ One disadvantage of XRD is the fact that data cannot be obtained at 2θ angles of less than about 1° , which corresponds to d_{001} around 8 nm. Thus XRD “sees” only intercalated clay and not exfoliated clay, and gives little indication of the relative amounts of each type. Transmission electron microscopy, on the other hand, gives a more direct visual indication of the state of the clay, including individual exfoliated layers and intercalated stacks.^{2,3} This gives a good qualitative picture, but to have a more quantitative overall measure of a sample it is necessary to perform a statistical average over a large number of analyses, a very time-consuming and expensive process.

Infrared (IR) spectroscopy is extensively used to characterize a wide range of materials, including layered silicates.⁴⁻⁷ It is surprising therefore that its use for characterizing nanoclay exfoliation seems to have been so little explored. We recently published a study in which IR spectroscopy was used to quantify the degree of orientation of both the polypropylene matrix and the reinforcing clay in blown nanocomposite films.⁸ In the course of that work, we became aware of the potential of this technique for obtaining information on the state of exfoliation in nanocomposites, and the purpose of this paper is to report our results on these films as well as on other samples that we subsequently examined. To our knowledge, there has been only one other report of similar findings.⁹

Layered silicates present a rather complicated subject for IR analysis.⁴⁻⁷ The silicon-oxygen stretching vibrational modes give rise to strongly absorbing bands in the $1100\text{-}1000\text{ cm}^{-1}$ region. Some of these involve the basal oxygens of the silicon-oxygen tetrahedra, i.e. they correspond to Si-O-Si linkages at the surface of the clay layers and have their transition moment (the direction of dipole oscillation during the vibration) lying in the plane of the layer; they are thus designated “in-plane”. Others involve the apical oxygens, i.e. they correspond to the Si-O⁻ bonds directed towards the octahedrally coordinated aluminum ions at the centre of the layer; these vibrations have their transition moment perpendicular to the layer and are designated “out-of-plane”. The intrinsically high absorptivity of these bands results in significant variations in the refractive index in this region, and consequently when the clays are

dispersed in a supporting medium for analysis, reflection at the clay-medium interface can complicate the spectrum and affect the overall band shape. Farmer and Russell have described how the spectrum depends on the type of clay as well as on the particle size and structure.⁴⁻⁷ In the case of Wyoming montmorillonite, for example, they observed four overlapping bands, three in-plane (1120, 1048, 1025 cm^{-1}) and one out-of-plane (1080 cm^{-1}).⁵ They reported that the position and sharpness of the out-of-plane mode “varies surprisingly with physical state”. For instance, it is particularly sensitive to particle size, and shows significant apparent shifts when the crystals are thinner than 100 nm. They attributed this behavior to the strong electric field produced by the oscillating Si-O⁻ dipoles, which causes the thin plates of the layer silicate crystals to become electrically polarized like the dielectric in a parallel-plate condenser.^{6,10} Furthermore, Russell and Farmer used IR spectroscopy to study the dehydration of montmorillonite and saponite via the water O-H stretching band around 3700-3000 cm^{-1} and the H-O-H bending band at 1640-1630 cm^{-1} .¹¹ They were able to distinguish two types of interlayer water, namely “firmly held” water molecules directly coordinated to the exchangeable cations and more labile water molecules in outer spheres of coordination. Thus changes in the interlayer spacing related to the loss of water could be correlated with IR results, and the shape of the Si-O stretching band envelope was also found to be affected. The swelling of clays with water was later studied in detail by Low and co-workers.¹²⁻¹⁶ Lerot and Low studied different montmorillonites swollen to varying degrees, and examined the effect on the shape of the Si-O stretching absorption.¹² They found that: (i) the frequencies of the four component peaks depended on the type of montmorillonite (degree of isomorphous substitution), but not on the water content; (ii) the out-of-plane mode became much more prominent with increasing water content, and the in-plane modes became narrower and more intense; (iii) the absorption coefficient for the principal Si-O absorption decreased with increasing isomorphous substitution but increased with increasing water content; and (iv) there was a rather abrupt change at a certain critical degree of swelling, which they attributed to a sudden rearrangement of the particles. For Upton montmorillonite with lithium or sodium as the interlayer cation, Zhang and Low established a clear linear correlation between the interlayer spacing, as measured by XRD, and the mass ratio of water

to clay, m_w/m_c .¹³ The position of the water H-O-H bending vibration was later shown to also vary with m_w/m_c .¹⁴ In a related study,¹⁵ the Si-O band envelope was analyzed in detail with the use of peak fitting to decompose it into its four components: Peak I ($\sim 1115 \text{ cm}^{-1}$), Peak II (the out-of-plane mode, $\sim 1080 \text{ cm}^{-1}$), Peak III ($\sim 1045 \text{ cm}^{-1}$), and Peak IV ($\sim 1024 \text{ cm}^{-1}$). The envelope clearly changes shape as m_w/m_c is varied from 0.71 (58% clay) to 42.8 (2% clay). Peak II, which can be barely seen at the lower water contents, becomes very visible as the interlayer spacing increases. In addition, the intensity ratio of Peak III to Peak IV increases. The positions of all four peaks shift as a function of m_w/m_c , but the greatest shift is observed for Peak II. The changes reach a plateau at $m_w/m_c \cong 6$, the point at which the spontaneous swelling of montmorillonite ceases and the interlayer distance is about 15 nm. It is interesting to note that this is well beyond the range that can be detected by XRD (about 8 nm). When water was replaced by NaCl or LiCl solutions of varying concentrations, no significant effect was observed.¹⁶ However, in a recent study in which the Fe^{3+} in the montmorillonite was reduced to Fe^{2+} , it was found that the iron oxidation state exerted a profound influence on the relationship between the water content and the position of the Si-O component peaks, and that the effect was reversible.¹⁷

Given these observations for water, similar behavior might be expected for other “swelling” media. In fact, such effects have been reported for hydrocarbon oil in a paper proposing the use of IR for characterizing the extent of dispersion of an organo-clay complex in the oil.¹⁸ It is therefore not surprising to find that it can also be applied to polymers, as will be demonstrated in this paper.

Experimental

The following nanoclays were obtained from Southern Clay Products, Inc.: Cloisite[®] Na⁺ (sodium montmorillonite, X-ray d_{001} 1.17 nm); Cloisite[®] 10A (intercalated with 39 % by weight dimethyl benzyl hydrogenated tallow quaternary ammonium, d_{001} 1.92 nm); Cloisite[®] 15A (intercalated with 43 % by weight dimethyl di(hydrogenated tallow) quaternary ammonium, d_{001} 3.15 nm); Cloisite[®] 20A (same intercalant at 38% by weight, d_{001} 2.42 nm); and Cloisite[®] 30B (intercalated with 30 % by weight methyl tallow bis-2-hydroxyethyl quaternary ammonium, d_{001} 1.85 nm). Nanomer[®] I.30E (intercalated

with 25-30 wt% octadecylamine) and Nanomer[®] I.28E (25-30 wt% trimethyl stearyl ammonium) were obtained from Nanocor, Inc.

Blown polypropylene (PP) films with and without nanoclay and compatibilizing agent were prepared and analyzed as described elsewhere.⁸ The constituents were polypropylene homopolymer (Pro-fax PDC1274 from Basell Polyolefins), Cloisite[®] 15A at a level of 2% by weight, and the following two maleic-anhydride-grafted polypropylene (MAGPP) compatibilizing agents: Epolene[®] 43 from Eastman Chemical Company, with a low molecular weight ($M_w = 9000$) but high MA content (3.8 wt%), and Polybond[®] 3150 from Chemtura Corp., with a high molecular weight ($M_w = 330,000$) and low MA content (0.5 wt%).

Blends of high density polyethylene (HDPE, Sclair[®] 2714 from Nova Chemicals) and maleic-anhydride-grafted HDPE (Polybond[®] 3009 from Chemtura Corp.) were prepared from cryogenically ground starting materials by processing at 190°C in a Haake “Minilab” twin-screw micro-extruder. The processed blends were also cryogenically ground. Nanocomposites containing 2% by weight of Cloisite[®] 20A were made from dry blends of the nanoclay with the ground blends or neat polymers, also by processing in the Haake extruder at 190°C. To obtain products with different states of intercalation/exfoliation, the materials were recirculated in the extruder for different periods of time ranging from 0 min (one pass straight through) to 30 min. Thin films for IR analysis and thicker samples for X-ray diffraction analysis were prepared by rapid hot pressing of the extrudate.

Infrared spectra were recorded on a Nicolet Magna 860 FT-IR instrument from Thermo Electron Corp. (DTGS detector, resolution 2 cm^{-1} , accumulation of 128 scans). Diffuse reflection spectra were measured with a “praying mantis” accessory from Harrick Scientific Corp. Peak fitting was performed with the use of GRAMS/AI software from Thermo Galactic Corp.

Results and Discussion

If the shape of the clay Si-O band envelope is to be considered for use as an indicator of clay intercalation in a polymeric matrix, it is first important to determine as a reference the spectrum for the

clay in its initial unintercalated and undispersed state, with as little perturbation as possible. This was done in two ways. In the first, the clay is dispersed in Nujol[®] mineral oil by light hand mixing with a mortar and pestle at room temperature, the mixture is sandwiched between potassium bromide windows with a 100 μm spacer, and the IR spectrum is measured in transmission. After the spectrum is converted to absorbance units, the Nujol peaks are eliminated by subtracting the spectrum of pure Nujol obtained in the same way. The result for 2 wt% Cloisite[®] Na⁺ (sodium montmorillonite) is shown in Figure 1. The difference spectrum clearly shows the usual montmorillonite absorption peaks, and the baseline is close to zero. In the second method, the clay is again hand mixed in a mortar and pestle, but this time with potassium bromide powder, and the spectrum is measured in diffuse reflection mode and ratioed against that of neat KBr. According to theory, after conversion to Kubelka-Munk units of $(1-R)^2/2R$, where R is the reflectance, the result should resemble the absorbance spectrum.

To check the effect of concentration, spectra of Cloisite[®] Na⁺ were measured by both methods at different concentrations. The resulting spectra in the Si-O stretching region are shown in Figure 2, both as recorded (Figs. 2a and 2b) and normalized to unit peak height to compare the band shapes (Figs. 2c and 2d). In Figure 2c, the four Si-O stretching modes are labelled I, II, III, and IV following the convention of Yan et al.¹⁵ (Peak II is not obvious because of overlap by the others.) The weaker peaks at 915, 880, and 845 cm^{-1} are librational modes of hydroxyl ions associated with two cations in the central octahedral layer, arising respectively from Al_2OH , $\text{Fe}^{3+}\text{AlOH}$, and MgAlOH groupings.⁴ The origin of the peak at 798 cm^{-1} is uncertain. In transmission, up to 4% concentration the overall band shape changes little, but at 6% it changes significantly. In diffuse reflection, the band shape is constant up to 2% but deviates significantly at 4% and 6%. In Figure 3 the peak heights are plotted against concentration for both methods. The relationship is linear up to 2% but deviations are observed at 4% and 6%, especially for diffuse reflection. We conclude that concentration effects are important, but can be minimized if transmission spectra are run at 4% or less and diffuse reflection spectra at 2% or less. However, even at these low levels, there is a significant difference between the transmission spectra and the diffuse reflection spectra. Although the peaks occur at much the same frequencies, the band

envelope has a different shape and is noticeably narrower in diffuse reflection than in transmission. This can be attributed to the different way in which reflection effects influence the spectra of these heterogeneous samples. Because the Si–O vibrations have very high intrinsic absorptivity, the refractive index in this region can be quite high, giving rise to a significant amount of reflection at the interface between the particles and the medium. This leads to multiple reflections within the sample, meaning that the effective path length is not constant. In transmission spectra, this is known to lead to an apparent “flattening” of peaks, a phenomenon sometimes known as the “wedging effect” because it occurs when the two faces of a sample or cell are not parallel.¹⁹

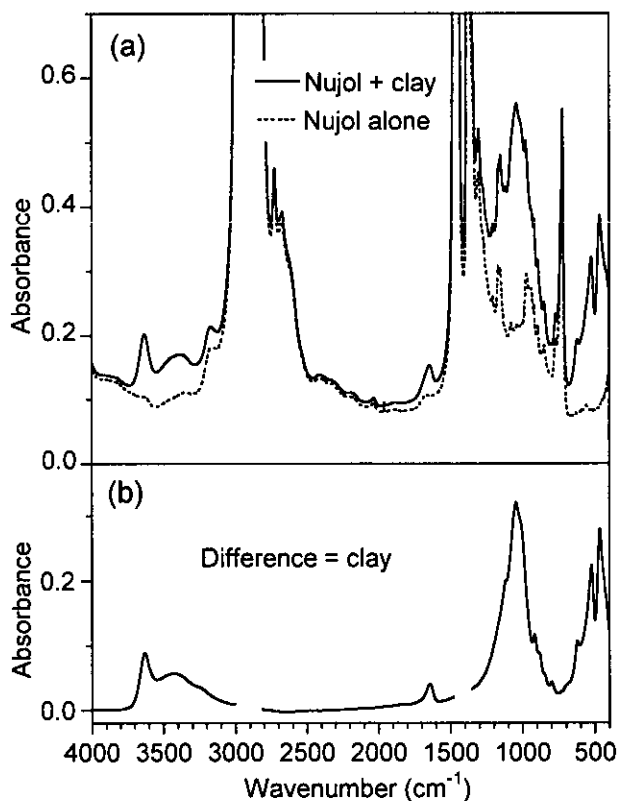


Figure 1. (a) IR transmission spectrum of Nujol containing 2 wt% of Cloisite[®] Na⁺ sodium montmorillonite clay (solid line), and the spectrum of Nujol alone (dotted line); (b) the difference spectrum obtained by subtraction, showing the clay absorption peaks. The blank spaces correspond to regions where the Nujol peaks are saturated.

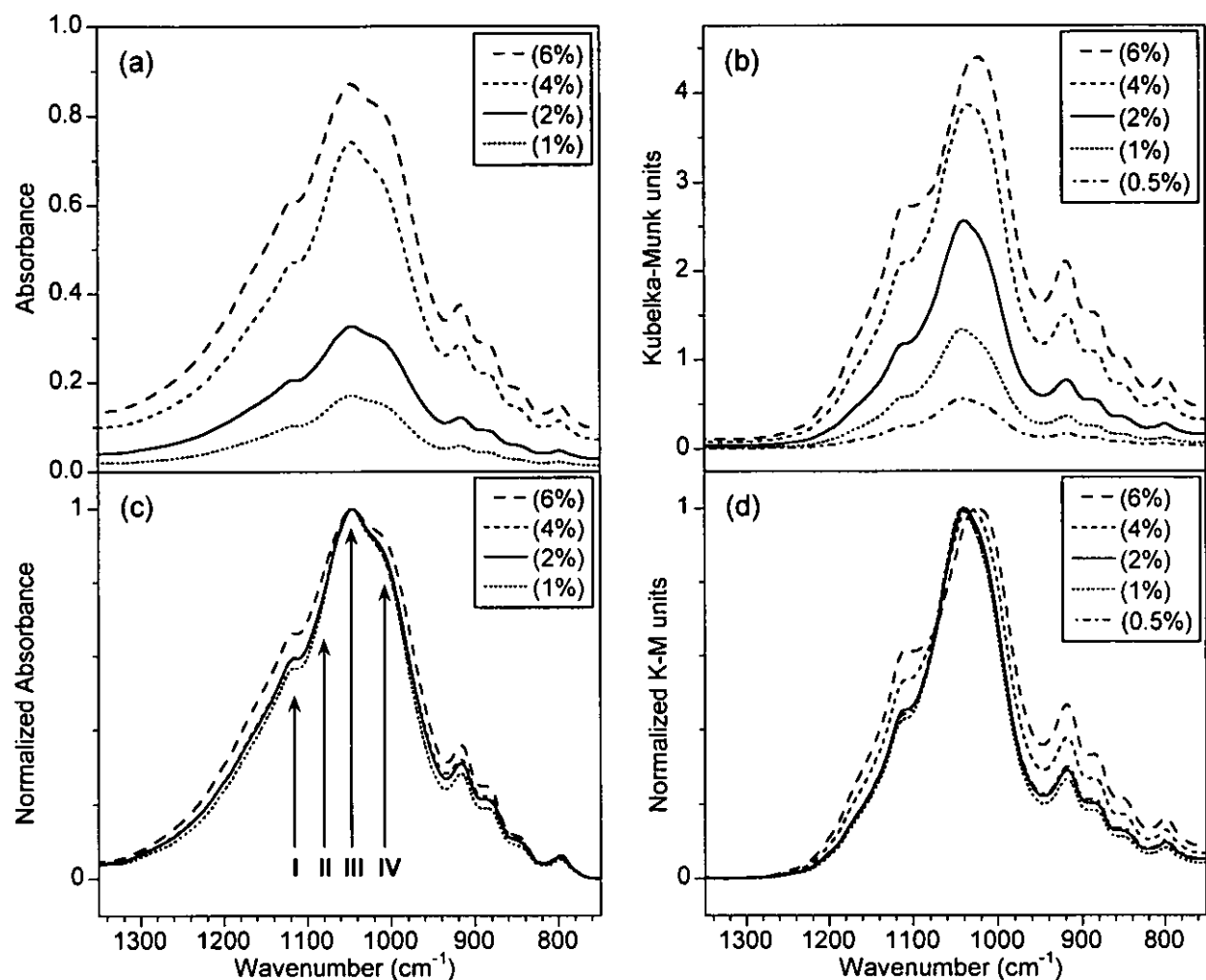


Figure 2. IR spectra in the Si–O stretching region of Cloisite[®] Na⁺ (sodium montmorillonite) clay: (a) spectra measured in transmission at different concentrations in Nujol, after subtraction of the Nujol spectrum; (b) spectra measured in diffuse reflection at different concentrations in KBr powder; (c) the transmission spectra normalized to unit peak height; (d) the diffuse reflection spectra normalized to unit peak height.

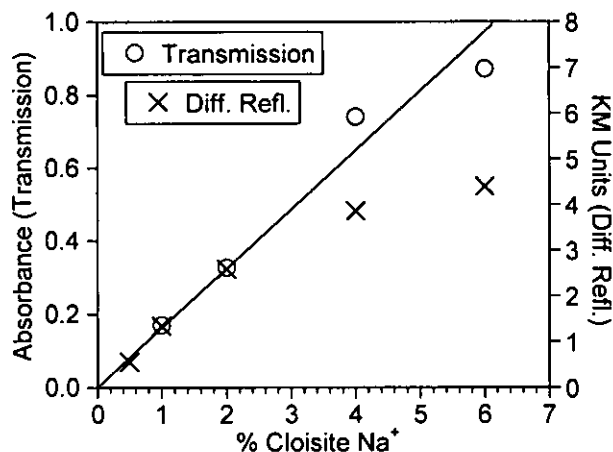


Figure 3. Relationship between peak height and concentration for the spectra of Figure 2.

Figure 4 compares the spectra of several different nanoclays measured in both transmission (2% in Nujol) and diffuse reflection (1% in KBr). The same trend is observed in both cases, namely a significant narrowing of the band envelope upon the introduction of organic intercalant between the clay layers of the sodium montmorillonite. In the case of the Cloisite[®] clays, Peaks I and III can be seen at 1120 and 1045 cm^{-1} respectively, with Peak IV as a shoulder near 1015 cm^{-1} . In the case of the Nanomer[®] clays, the shape of the envelope is significantly different; Peaks I, III, and IV have all shifted downwards by about 10 cm^{-1} , whereas Peak II has shifted upwards and can now be seen more clearly around 1085 cm^{-1} . This difference can very probably be attributed to the different origins of the two montmorillonites. The peak at 880 cm^{-1} is noticeably weaker in the Nanomers than in the Cloisites, which suggests that the Nanomers contain a lower amount of Fe^{3+} . This would explain the differences in the overall band shape, because Yan and Stucki observed exactly the same changes when the Fe^{3+} ions in sodium-saturated Upton montmorillonite were reduced to Fe^{2+} .¹⁷ Figure 4 confirms that the Si-O stretching band envelope is affected by both the chemistry of the montmorillonite and the presence of intercalant.

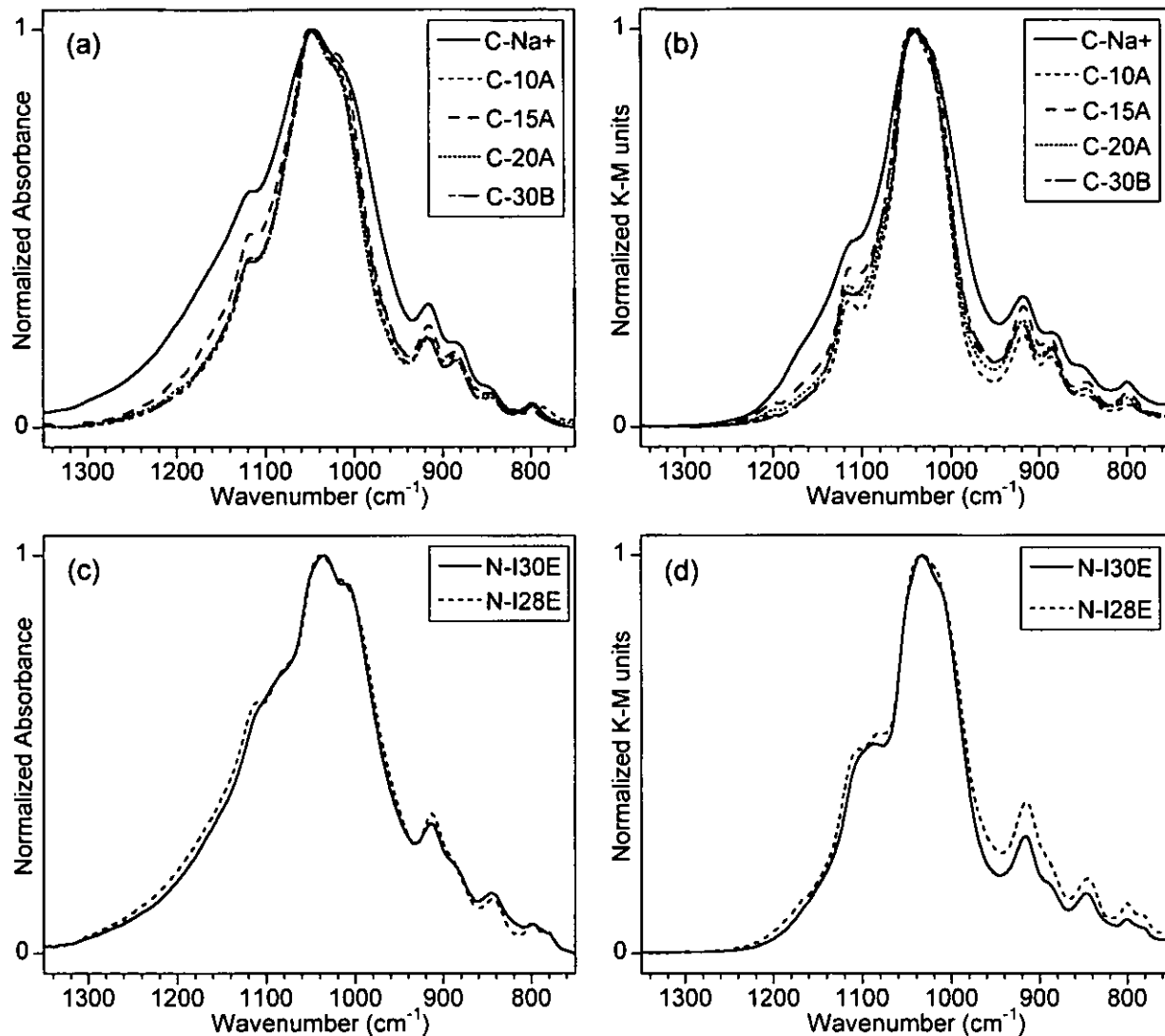


Figure 4. IR spectra of different clays, normalized to unit peak height for comparison: (a) Cloisite[®] clays at 2% in Nujol, transmission; (b) Cloisite[®] clays at 1% in KBr, diffuse reflection; (c) Nanomer[®] clays at 2% in Nujol, transmission; (d) Nanomer[®] clays at 1% in KBr, diffuse reflection.

It is well known that orientation can also profoundly affect the band shape, because the intensity of the IR absorption is proportional to the square of the dot product of the vectors corresponding to the transition moment of the vibration and the electric field of the radiation, i.e. to the square of the cosine of the angle between the two. Thus if the clay layers are aligned perpendicular to the IR beam direction, the in-plane modes (Peaks I, III, and IV) will be enhanced while the out-of-plane mode (Peak II) will be diminished.⁴ This can be clearly seen in Figure 5, taken from our earlier work on blown PP films

containing 2 wt% of the nanoclay Cloisite 15A.⁸ It shows the spectra of a film with the composition 78% PP, 2% Cloisite[®] 15A, and 20% of the compatibilizing agent Polybond[®] 3150. The spectra labelled “MD” and “TD” were measured with the film perpendicular to the beam and with polarization in the machine direction and the transverse direction, respectively. Because of strong clay layer orientation in the plane of the film, the in-plane modes III and IV are quite strong while the out-of-plane mode II is very weak. The spectrum labelled “ND” corresponds to polarization in the normal or thickness direction of the film. Since the spectrum cannot be easily measured with the film turned by 90° with respect to the beam, the ND spectrum is obtained by tilting the film at 45° and then correcting for the contribution of the MD or TD spectrum. The ND spectrum is quite different from the MD and TD spectra; the out-of-plane mode is now quite prominent while the in-plane modes are very weak. The structural factor spectrum SF is obtained by taking the average of the other three. It corresponds to the spectrum that would be obtained if there were no orientation in the sample. It should be noted that measuring the spectrum without polarization does not give the SF spectrum; instead it gives the average of the MD and TD spectra, which can be quite different.

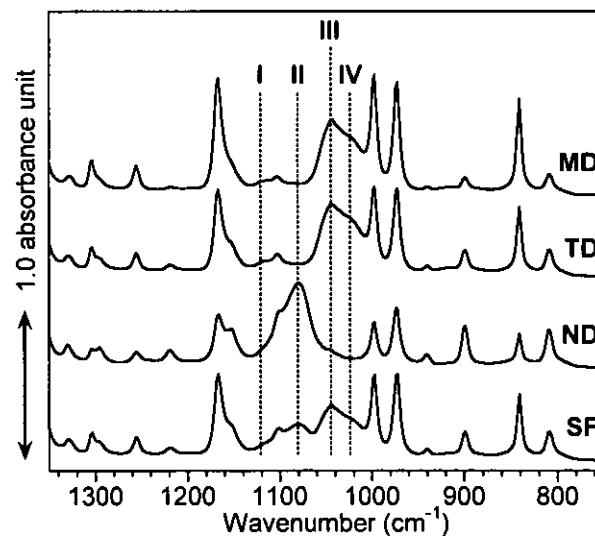


Figure 5. IR spectra (offset along the y-axis for clarity) of a blown PP nanocomposite film corresponding to polarization in the machine direction (MD), the transverse direction (TD), and the normal direction (ND), along with the structural factor spectrum (SF). Peaks I to IV are the Si-O stretching modes of the clay.

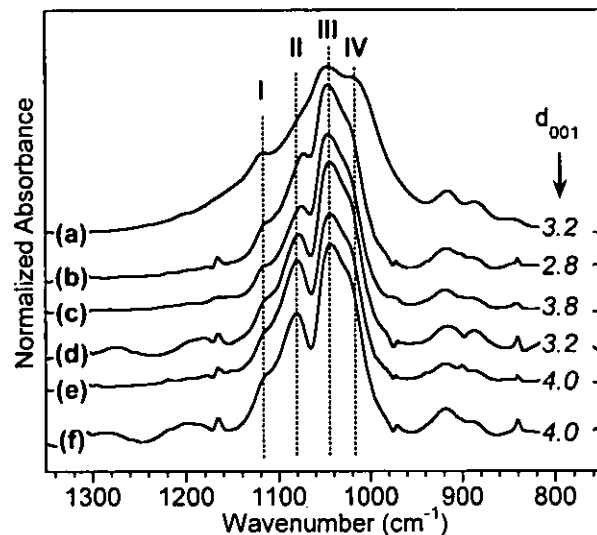


Figure 6. IR spectra of 2% Cloisite 15A: (a) dispersed by hand in Nujol; (b-f) in PP nanocomposite films containing different compatibilizing agents: (b) none; (c) 4% Epolene 43; (d) 4% Polybond 3150; (e) 20% Polybond 3150; (f) 38% Polybond 3150. The interlayer spacings d_{001} (in nm) corresponding to the maxima of the peaks in the XRD curves are shown on the right.

In our earlier publication, we considered only the orientation in the blown films and did not report on other aspects. To do this, we now consider the structural factor spectra of the different films, which are free of orientation effects. These are shown in Figure 6 along with the spectrum of Cloisite 15A dispersed by hand in Nujol for comparison. The thickness of the films was such that the measured absorbance never exceeded 1.1 below 1350 cm^{-1} . To better see the clay peaks, the spectrum of the PP matrix has been subtracted in the same way described for Nujol. In the case of PP, the subtraction sometimes leaves small residual features, probably because of slight crystallinity differences. Interference fringes also appear in some spectra. However, the variations in the shape of the clay band envelope are clearly evident. Compared to the unprocessed clay (Fig. 6a), clay that has been processed with PP in the extruder (Figs. 6b to 6f) gives a narrower band envelope and shows a visible Peak II. Even without compatibilizing agent, this peak can be seen, at 1075 cm^{-1} (Fig. 6b). When 4% Epolene 43 is present in the composition, it becomes more obvious and shifts to 1077 cm^{-1} (Fig. 6c). With 4% Polybond 3150 instead of Epolene 43, it becomes still more obvious and shifts to 1079 cm^{-1} (Fig. 6d).

The trend continues if the concentration of Polybond is increased, with Peak II continuing to shift slightly to 1080 cm^{-1} (Fig. 6e) and 1081 cm^{-1} (Fig. 6f). This apparent growth and/or shift of Peak II is very similar to that observed for swelling with water.¹⁵ It seems reasonable, therefore, to associate this trend with increasing efficiency of intercalation/exfoliation, and the XRD data included in Figure 6 tend to support this to a certain extent. If we consider only the PP films with Polybond concentrations of 0, 4, 20, and 38%, the trend is clear ($d_{001} = 2.8, 3.2, 4.0, 4.0\text{ nm}$) and follows the IR results. The results for the starting clay and the film containing Epolene do not follow the IR trend exactly, however. One possible explanation for this is that the chemistry of the intercalant has an influence on the spectrum. Although Epolene and Polybond are both MAgPPs, Epolene has much higher MA content and much lower molecular weight. Another possible cause is the difficulty in correlating the XRD and IR data. It must be remembered that the clay layer spacing is by no means uniform, but is distributed over a wide range of values, possibly including the state of complete exfoliation. The maximum of the XRD curve is a measure only of the most probable spacing, and while the shape of the curve gives some idea of the distribution, XRD cannot give reliable data below 2θ about 1° , or $d_{001} > 8\text{ nm}$. The IR response, on the other hand, is an average over all the clay present, including particles beyond the range of XRD. For this reason, it would be a more reliable indicator of the overall extent of intercalation/exfoliation.

To explore the potential of IR analysis in greater depth, a more systematic study was undertaken on high density polyethylene (HDPE), the maleated HDPE Polybond[®] 3009, and blends thereof with Polybond contents of 1, 2, 33, and 67 % by weight. As described in the Experimental section, Cloisite 20A nanoclay was dispersed in each matrix at a level of 2 wt % in a micro-extruder at 190°C for different processing times, and from the extrudate, thick and thin films were prepared by rapid hot pressing for XRD and IR analysis respectively. Unlike the blown films, these pressed films were analyzed without polarization and tilting to correct for orientation effects, as this would have required considerable extra effort. A few of the films were analyzed in this way, and although it was found that the pressing induced some clay orientation, the degree was significantly lower than in the blown films (Hermans orientation function around 0.3 as compared to 0.8) and fairly reproducible. Hence it was felt

that the orientation effects could be considered as a constant factor that would not interfere with the comparison of the spectra, which are shown for four of the compositions in Figure 7 along with the reference spectrum of Cloisite 20A measured in Nujol. As in the previous examples, the spectrum of the polymer matrix has been subtracted.

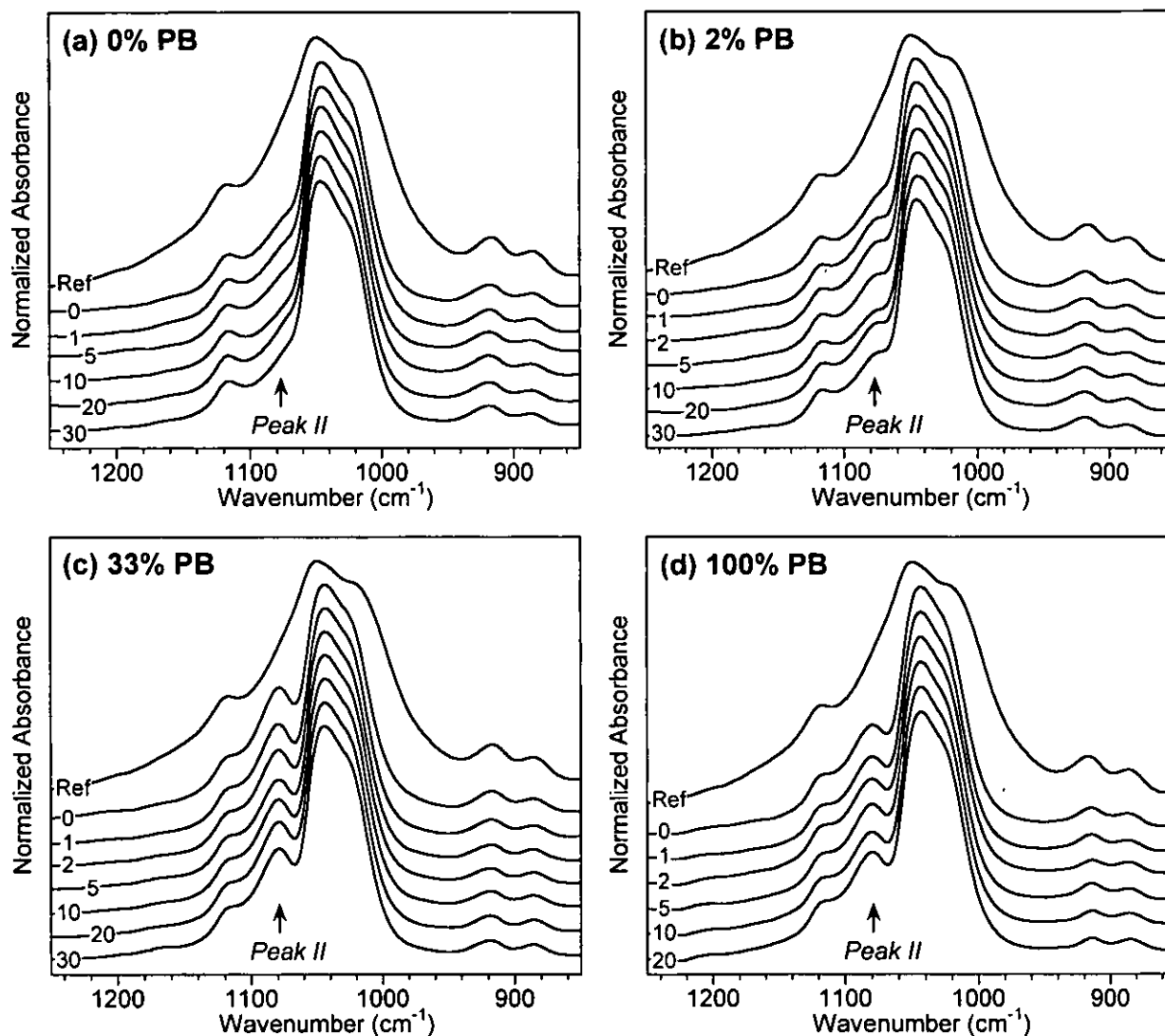


Figure 7. IR spectra of 2% Cloisite 20A dispersed by hand in Nujol (“Ref”) or processed in HDPE containing different amounts of Polybond 3009 (indicated at the top left of each graph) for different recirculation times in minutes (indicated at the bottom left of each graph).

The first observation is that no matter what the matrix composition, just one pass through the micro-extruder (0 min recirculation) results in substantial narrowing of the band envelope compared to the unprocessed clay. In the case of pure HDPE (Fig. 7a), Peak II becomes somewhat more evident at this

point but does not appear to evolve much more with further recirculation. With 2% Polybond in the PP matrix (Fig. 7b), after one pass the spectrum is similar to the one for no Polybond, but after recirculation for 1 min it becomes more prominent, then seems to remain stable. When the Polybond content is 33%, Peak II is much more prominent even after one pass, and then remains stable. Much the same is true for 100% Polybond. If the IR spectrum is an indication of intercalation/exfoliation, a stable state seems to be attained rather quickly, and although this state depends on the concentration of compatibilizing agent up to a certain level, beyond that there seems to be little effect.

It is obviously of interest to quantify these changes in the clay spectrum so as to be able to compare the state of exfoliation in different samples. This is not an easy task. In an attempt to do so, we have applied peak fitting to the spectra in order to better understand the changes that are occurring, but again, this is not easy. There are always important questions concerning the choice of lineshape and the number of peaks to use. While the theory-based Lorentzian lineshape works well in many cases, like liquids and well-ordered solids, it does not necessarily work so well in the case of a less-well-structured solid like the naturally occurring layered silicates. This is because the clay particles comprise a distribution of structures and environments with slightly different vibrational frequencies, so that the overall IR absorption band can be considered as the superposition of a distribution of Lorentzian peaks. This introduces Gaussian character into the lineshape. To deal with this situation, we have used the well known Pearson VII lineshape function,^{20,21} which includes an adjustable parameter m that allows the lineshape to vary from purely Lorentzian ($m = 1$) to purely Gaussian ($m = \infty$). After trials with a number of spectra, we found $m = 4$ (about 75% Gaussian character) to be the best value for general use. It was assumed that the lineshape is the same for all peaks in the spectrum, which is not necessarily entirely true. However, if the lineshape is allowed to vary in the fit along with the other parameters (peak position, width, and height), then there are too many variables and it is impossible to obtain a reliable convergent fit.

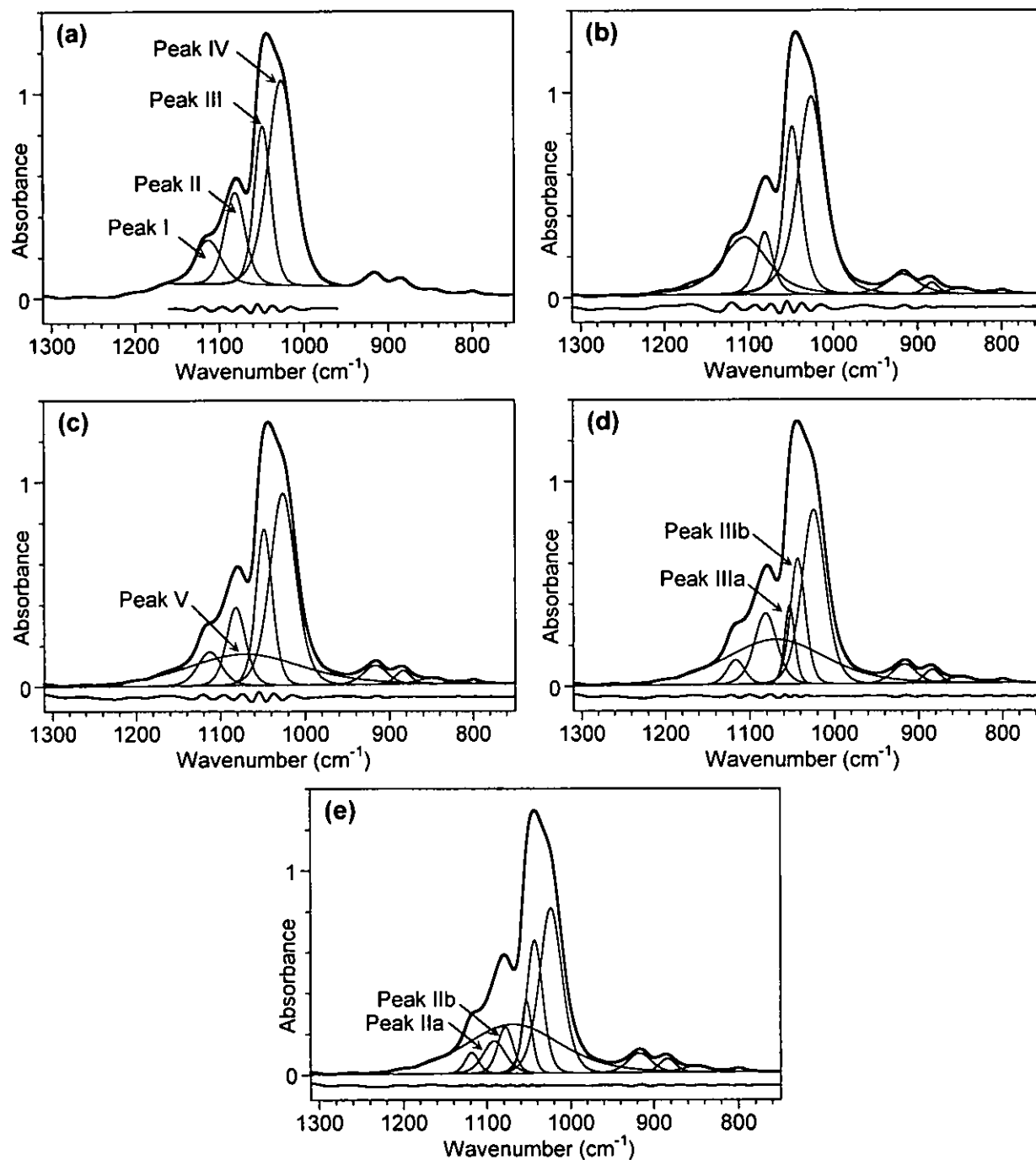


Figure 8. Peak fits of the clay band envelope for 2% Cloisite 20A in 2:1 Polybond:HDPE at 20 min recirculation time: (a) fit with four peaks from 1160-960 cm^{-1} only; (b) fit of complete band envelope with eight peaks; (c) fit with nine peaks; (d) fit with ten peaks; (e) fit with eleven peaks. The curve of intermediate thickness at the bottom of each graph corresponds to the residual difference between the experimental spectrum (thick line) and the sum of the fitted peaks (thin lines). It is displaced downwards from zero for greater visibility.

Figure 8 shows some results obtained for a typical spectrum (2% Cloisite 20A in 2:1 Polybond:HDPE at 20 min recirculation time). We began with the approach used by Yan et al., namely fitting the 1160-960 cm^{-1} region with four peaks and a linear variable baseline.¹⁵ Although this approach served their purpose quite well, it can be seen from the residual curve in Figure 8a that in the present case there is room for improvement. The fit should really comprise the whole band envelope, including the four weaker peaks at lower wavenumber. When this is done, the best result that could be obtained with eight peaks is shown in Figure 8b. It is clearly inadequate. Changing the value of m did not improve the fit significantly, and in fact a Lorentzian lineshape gave the worst result. When a ninth peak was added, the best result was obtained with a very broad underlying peak that we designate Peak V, as shown in Figure 8c. This is better than Figure 8b, but still inadequate, and again changing the lineshape gave no significant improvement. A more reasonable fit was obtained on adding a tenth peak, as shown in Figure 8d. This amounts to splitting Peak III into two components, designated Peaks IIIa and IIIb. However, the most acceptable fit was obtained with eleven peaks, as shown in Figure 8e, where Peak II is also split into two components, Peaks IIa and IIb. Thus, in the best fit, Peaks II and III seem to consist of two components. It should be stressed that this approach to the peak fitting is not based only on the spectrum shown in Figure 8, but on trials with a number of spectra measured for different Cloisites processed under different conditions in different polymers and in mineral oil. Although the origin of the “new” peaks is not entirely clear, they represent real effects. In the case of Peaks II and III, the two components are probably not different vibrational modes, but are required to account for an asymmetry of the peak that arises from an asymmetric distribution of environments in the sample. For Peak II, this asymmetry can be seen in the ND spectra of oriented samples, where the peak stands out clearly. It can be seen, for example, in Figure 5, in spite of the presence of the small superimposed PP peak at 1103 cm^{-1} . In our earlier work on orientation,⁸ the trichroic spectra were analyzed by peak fitting with the inclusion of Peaks IIa, IIb, IIIa, and IIIb. The average respective dichroic ratios $A_{\text{par}}/A_{\text{perp}}$ for the five films (which showed similar orientation) were found to be 0.13, 0.05, 2.94, and 2.60, where “parallel”

and “perpendicular” refer to the direction of the polarization with respect to the plane of the film. This confirms that both Peaks IIa and IIb show similar “out-of-plane” dichroism, whereas Peaks IIIa and IIIb show similar “in-plane” dichroism, the opposite of Peaks IIa and IIb. The broad underlying peak V is more difficult to explain. It is very likely not a true vibrational mode, but rather a somewhat empirical means of dealing with the broadening of the band envelope caused by the optical effects mentioned earlier. It should be stressed that it was impossible to account for these effects by varying the width or lineshape of the other peaks, unless an unduly large number of peaks were introduced. Since such effects are related to the degree of dispersion of the clay, it is important to treat them in the analysis, even though a rigorous approach is not possible because of the complexity of the situation.

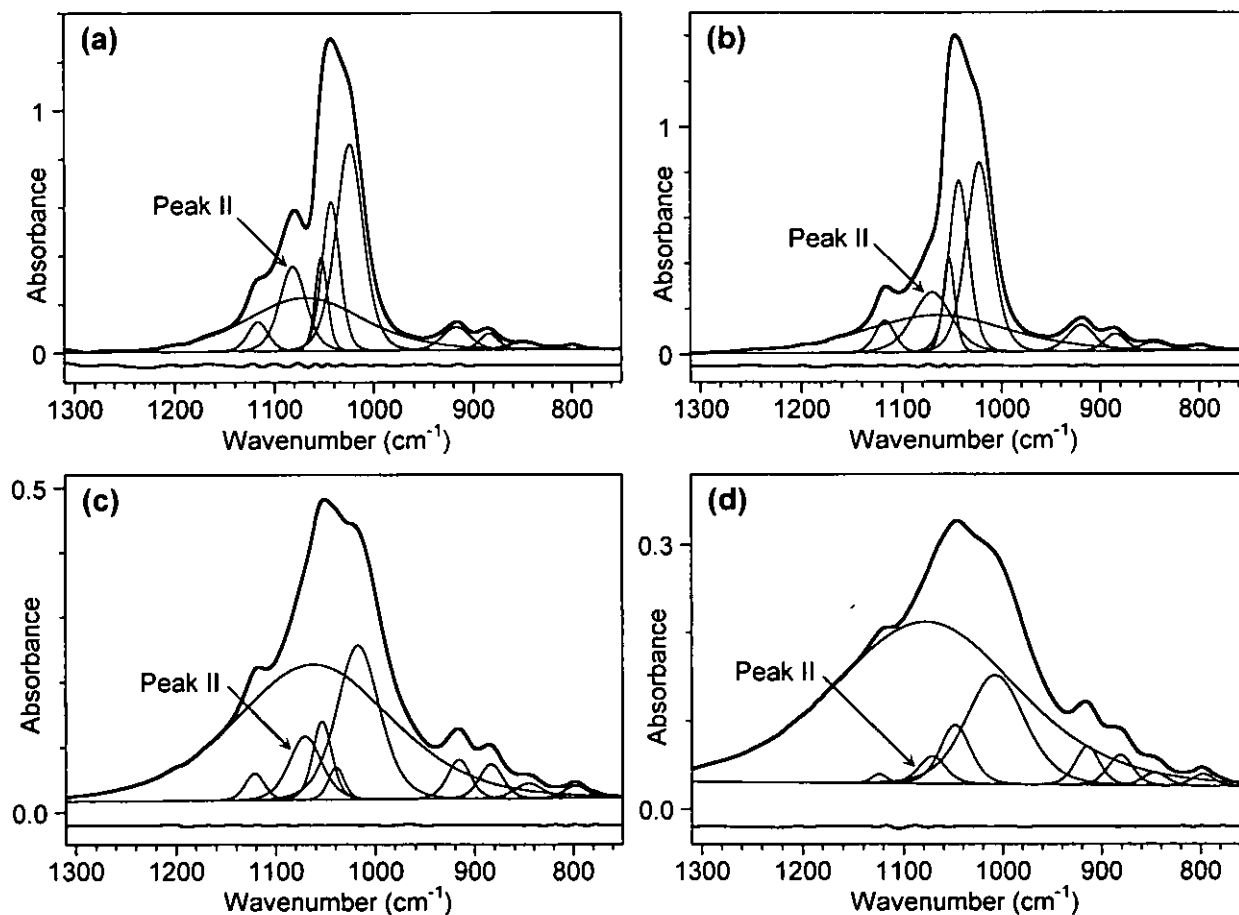


Figure 9. Examples of peak fits of different clay spectra: (a) 2% Cloisite 20A in 2:1 Polybond:HDPE at 20 min recirculation time; (b) 2% Cloisite 20A in HDPE alone at 30 min recirculation time; (c) 2% Cloisite 20A in Nujol®; (d) 2% Cloisite Na⁺ in Nujol®.

Although the fit with eleven peaks shown in Figure 8e can be successfully used in many cases, this is not always true. Problems arise when Peak II does not stand out clearly and is “hidden” under the other peaks. In such cases, Peaks IIa and IIb cannot be unequivocally determined by the peak fitting process. Thus, as a general approach, we decided to use a total of ten peaks, that is, to represent Peak II by one component only, even if this is an approximation. Figure 9 compares examples of different spectra analyzed with this approach. Figure 9a is the case already discussed. The “waviness” of the residual curve in the region of peak II confirms that the fit is not perfect with ten peaks, but nevertheless it is reasonably good. Figure 9b is a spectrum obtained with HDPE alone, where Peak II is less evident. In this case, the fit with ten peaks is better than in Figure 9a, and if an extra peak is added to the fit, problems with convergence result. Figure 9c is the spectrum of Cloisite 20A in Nujol. The much larger overall band width in this case is accounted for by a stronger Peak V. Peaks I, II, IIIa, IIIb, and IV are still well determined, although the relative intensities of Peaks IIIa and IIIb have changed somewhat. Finally, Figure 9d shows the spectrum of the unintercalated clay Cloisite Na⁺, in which the absorption band is quite broad. Nevertheless, the fit still works well, although in this case only one component was required for Peak III as well as for Peak II.

Having developed this peak fitting protocol, which we stress again was found to work well for a wide variety of clay spectra, we then applied it to the series of spectra shown (in part) in Figure 7. The data were then analyzed closely to determine which parameters are most sensitive to the matrix and the processing. As expected, Peak II was particularly sensitive. Both the peak position and the width at half height change with processing, as shown in Figure 10. For the pure HDPE, the position remains close to that of the starting clay (1070 cm⁻¹) and the peak remains hidden under Peaks III and IV. As a result, its position and width are harder to determine with precision and the variations seen in Figure 10 may not be significant. For the blends containing Polybond, however, the situation is more clear. At 1% Polybond, Peak II shifts to 1072.5 cm⁻¹ after one pass through the extruder, then to 1074.4 and 1076.4 cm⁻¹ after 1 and 2 minutes respectively of recirculation. At this point the system appears to reach a steady state. With 2% Polybond, the changes occur somewhat faster, with the peak shifting to 1076.2

cm^{-1} after only 1 minute of recirculation and then reaching a plateau around 1077.1 cm^{-1} , slightly higher than at 1%. When the Polybond concentration is very high, the steady state is reached after only one pass, and the plateau values are higher still: 1080.6 cm^{-1} at 33% Polybond, 1081.0 cm^{-1} at 67% Polybond, and 1081.5 cm^{-1} at 100% Polybond. It should be noted that these values are the same as those found for high concentrations of compatibilizing agent in the blown PP films. The increase in the frequency of Peak II is accompanied by a parallel decrease in the peak width, as shown in Figure 10b. In fact, there is a reasonably good linear correlation between the two, as shown in Figure 10c. These changes obviously reflect the influence of clay intercalation and exfoliation on the out-of-plane Si-O⁻ mode. They are related to the changes in the distribution of environments of the Si-O⁻ bonds, and as already mentioned, this distribution may take on some degree of asymmetry. Under the conditions used in this experiment, the intercalation seems to take place rather quickly and an equilibrium state is reached within a few minutes.

Figure 11 shows two other parameters, based on peak areas, that are sensitive to the processing. To avoid any dependence on the overall spectral intensity, we use the ratio of peaks within the same spectrum. One parameter (Fig. 11a) is the ratio of the area of Peak III (the sum of IIIa and IIIb) against the area of Peak IV. This ratio increases rapidly with processing for the first five minutes or so, then reaches a steady state. Again, the steady state level seems to correlate with the Polybond concentration, although not quite as well as it does for the Peak II position. The ratio of Peak II to Peak IV was also examined, but it did not change as much. Thus the increasing prominence of Peak II upon processing is due mainly to the shift to higher wavenumber, and not to an increase in relative intensity. It is worth repeating here that Yan et al.,¹⁵ in their study of water swelling of montmorillonite, also found that the position of Peak II and the ratio of Peak III to Peak IV varied in a manner similar to that seen here. Another parameter that is sensitive to the processing (Fig. 11b) is the ratio of the area of the broad underlying Peak V against the sum of Peaks I to IV. It also changes rapidly within the first few minutes, although in this case it decreases as the band envelope narrows. It is interesting to note that in this case,

although the initial rate of change depends on the Polybond concentration, the ultimate value reached is much less sensitive.

It would obviously be useful to have data from other techniques to support our conclusions. Although quantitative data on the state of intercalation/exfoliation is not readily available, the X-ray diffraction data obtained on our extruded samples do provide some support. The samples containing 2% Polybond or less all showed a clear intercalation peak. Samples with a high Polybond content, on the other hand, showed either no peak or only a very weak one, indicating a much better state of exfoliation. The corresponding d-spacing values determined where possible are given in Table 1. The d-spacing for the starting clay was 2.4 nm. Apart from somewhat anomalous values for the 2% Polybond sample, they follow a logical trend. For a recirculation time of 0 min (one pass through the extruder) they increase with Polybond concentration, from 3.08 nm at 0% to 3.48 nm at 100%. For 0% and 1% Polybond, they also increase with recirculation time, as expected, up to 5 min. Beyond this they appear to decrease, but there is a plausible explanation for this, namely that the clay stacks with larger d-spacings, corresponding to the low angle side of the peak, are being preferentially exfoliated, leaving behind the stacks with smaller spacings and thus shifting the peak maximum to a lower d-spacing value. This underlines the problem of trying to correlate the peak maximum, which is a rather limited measure of the overall state of exfoliation, with the infrared data, which represents an average over the entire sample. In fact, infrared spectroscopy is probably the better technique for obtaining a complete and quantifiable measure of the state of intercalation. Furthermore, it has the potential to be applied as a relatively fast and easy quality control method. On-line application to polymer melts can also be envisaged, for example through the use of attenuated total reflection (ATR), and in fact our ongoing work is providing support for the potential of this approach.

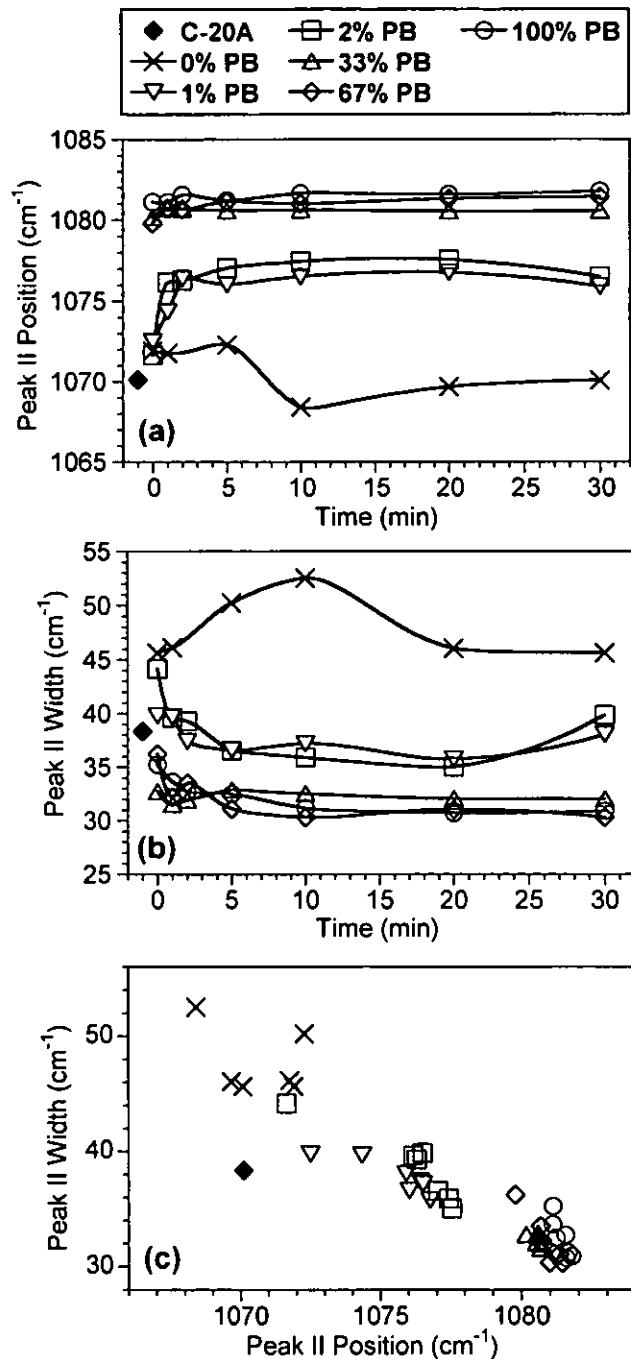


Figure 10. Peak II parameters determined by peak fitting for Cloisite 20A in blends of Polybond 3009 (PB) and HDPE with varying percentages of PB: (a) peak position in cm⁻¹ as a function of recirculation time; (b) width at half height in cm⁻¹ as a function of recirculation time; (c) relationship between peak position and width. The legend for the symbols is shown at the top of the figure. The C-20A data point (◆) corresponds to the reference spectrum recorded in Nujol.

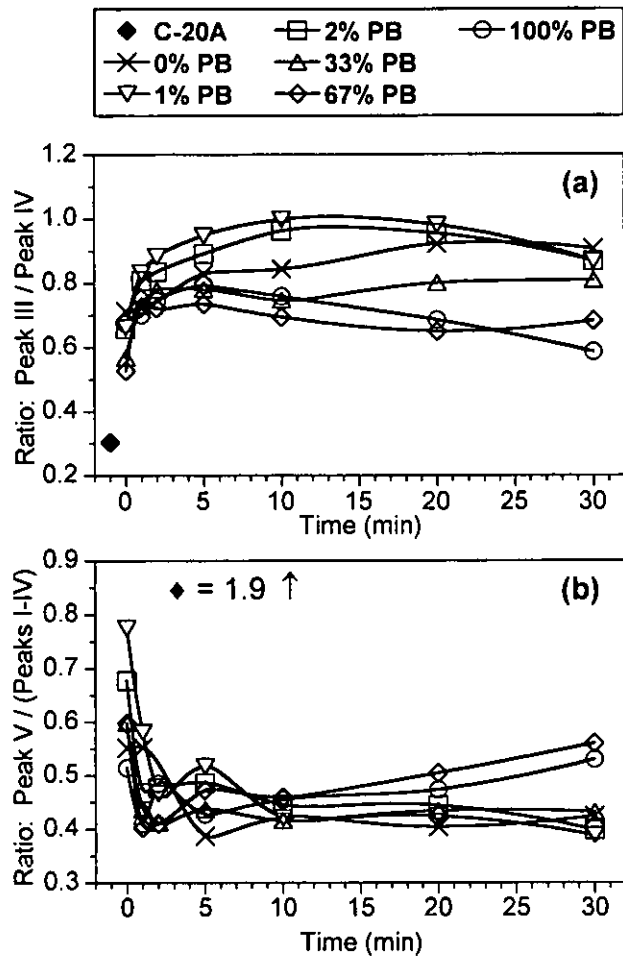


Figure 11. Parameters determined by peak fitting for Cloisite 20A in blends of Polybond 3009 (PB) and HDPE with varying percentages of PB: (a) ratio of the area of Peak III with respect to that of Peak IV; (b) ratio of the area of the broad underlying Peak V with respect to the sum of Peaks I-IV. The legend for the symbols is shown at the top of the figure. The C-20A data point (\blacklozenge) corresponds to the reference spectrum recorded in Nujol.

Conclusion

The potential of infrared spectroscopy as a method for characterizing the state of intercalation/exfoliation in polymer nanocomposites containing montmorillonites has been clearly demonstrated. The shape of the clay absorption envelope at $1300\text{-}750\text{ cm}^{-1}$ changes as a function of processing and this presumably results from better intercalation and exfoliation. This is supported by

X-ray diffraction results. When peak fitting was applied to better understand the reasons for the changes, two main factors were identified. The first is a change in position and width of the peak arising from the out-of-plane Si-O⁻ vibrational mode, both of which change with processing until a steady state is reached. The position of the peak in this steady state is dependent on the amount of compatibilizing agent present in the material. At this point it is not clear whether this is solely due to physical effects (increasing interlayer distance), or whether the chemistry of the compatibilizing agent also plays a role. The presence of a higher amount of polar maleic anhydride groups may result in enhanced interaction with the Si-O⁻ dipoles. The second factor is a narrowing of the overall band envelope that may be represented by the diminishing contribution of a broad underlying peak. Our ongoing work indicates that similar changes occur in other polymers like polystyrene, polyamides, and epoxy resins. Other ongoing work is being devoted to other types of clays and to model studies in mineral oil in order to better understand the origins of these changes.

Acknowledgement. This work was supported by the members of the “PNC-Tech” industrial technology group, and we thank them for their support and the permission to publish. Thanks are also due to Ms. Dominique Desgagnés for her careful work in recording many infrared spectra, to Ms. Chantal Coulombe for the preparation of samples in the micro-extruder, and to Ms. Florence Perrin-Sarazin and Ms. Geneviève Dorval-Douville for supplying the blown PP films.

References

1. Vaia, R. A.; Liu, W. *J. Polym. Sci.: Part B: Polym. Phys.* **2002**, *40*, 1590-1600.
2. Morgan, A. B.; Gilman, J. W.; Jackson, C. L. *Macromolecules* **2001**, *34*, 2735-2738.
3. Drummy, L. F.; Koerner, H.; Farmer, K.; Tan, A.; Farmer, B. L.; Vaia, R. A. *J. Phys. Chem. B* **2005**, *109*, 17868-17878.

4. Farmer, V. C. In *The Infrared Spectra of Minerals*; Farmer, V. C., Ed.; Mineralogical Society, London, 1974; Chapter 15, pp. 331-363.
5. Farmer, V. C.; Russell, J. D. *Spectrochim. Acta* **1964**, *20*, 1149-1173.
6. Farmer, V. C.; Russell, J. D. *Spectrochim. Acta* **1966**, *22*, 389-398.
7. Farmer, V. C.; Russell, J. D. In *Clay Mineralogy: Spectroscopic and Chemical Determinative Methods*; Wilson, M. J., Ed.; Chapman & Hall, London, 1994; Chapter 2, pp. 11-67.
8. Cole, K. C.; Perrin-Sarazin, F.; Dorval-Douville, G. *Macromol. Symp.* **2005**, *230*, 1-10.
9. Ijdo, W. L.; Kemnetz, S.; Benderly, D. *Polym. Eng. Sci.*, **2006**, *46*, 1031-1039.
10. Farmer, V. C.; Russell, J. D. *Clays Clay Miner.* **1967**, *15*, 121-142.
11. Russell, J. D.; Farmer, V. C. *Clay Miner. Bull.* **1964**, *5*, 443-464.
12. Lerot, L.; Low, P. F. *Clays Clay Miner.*, **1976**, *24*, 191-199.
13. Zhang, Z. Z.; Low, P. F. *J. Colloid Interface Sci.*, **1989**, *133*, 461-472.
14. Yan, L.; Low, P. F.; Roth, C. B. *Clays Clay Miner.*, **1996**, *44*, 749-756.
15. Yan, L.; Roth, C. B.; Low, P. F. *Langmuir*, **1996**, *12*, 4421-4429.
16. Yan, L.; Roth, C. B.; Low, P. F. *J. Colloid Interface Sci.*, **1996**, *184*, 663-670.
17. Yan, L.; Stucki, J. W. *Langmuir*, **1999**, *15*, 4648-4657.
18. Schaefer, F. W.; Wright, A. C.; Granquist, W. T. *NLGI Spokesman*, **1971**, *34*, 418-423.
19. Cole, K. C.; Pilon, A.; Noël, D.; Hechler, J.-J.; Chouliotis, A.; Overbury, K. C. *Appl. Spectrosc.*, **1988**, *42*, 761-769.

20. Heuvel, H. M.; Huisman, R.; Lind, K. C. J. B. *J. Polym. Sci.: Polym. Phys. Ed.*, **1976**, *14*, 921-940.

21. Heuvel, H. M.; Huisman, R. *J. Appl. Polym. Sci.*, **1985**, *30*, 3069-3093.

Table 1. Clay interlayer spacings in nm determined by XRD for extruded samples of blends of Polybond 3009 and HDPE containing 2% Cloisite 20A.

Recirculation Time (min)	Polybond Content (%)					
	0	1	2	33	67	100
0	3.08	3.11	3.67	3.27	3.37	3.48
1	3.15	3.30	3.24	—	—	—
2	3.27	3.34	3.15	—	—	—
5	3.37	3.39	—	—	—	—
10	3.04	3.08	3.14	—	—	—
20	3.21	3.13	3.09	—	—	—
30	3.16	3.48	3.53	—	—	—

The Use of Infrared Spectroscopy to Characterize Clay Intercalation and Exfoliation in Polymer Nanocomposites

K. C. Cole

